New substituted imidazo[1,5-a]pyridine and imidazo[5,1-a]isoquinoline derivatives and their application in fluorescence cell imaging

Giorgio Volpi, Beatrice Lace, Claudio Garino, Emanuele Priola, Emma Artuso, Paolo Cerreia Vioglio, Claudia Barolo, Andrea Fin, Andrea Genre, Cristina Prandi.

New substituted imidazo[1,5-a]pyridine and imidazo[5,1-a]isoquinoline derivatives and their application in fluorescence cell imaging.

Dyes and Pigments, 157, 2018, pagg. 298-234.

DOI: 10.1016/j.dyepig.2018.04.037

New substituted imidazo[1,5-a]pyridine and imidazo[5,1-a]isoquinoline derivatives and their application in fluorescence cell imaging

G. Volpi[a], B. Lace[b], C. Garino[a*], E. Priola[a], E. Artuso[a], P. Cerreia Vioglio[c], C. Barolo[a], A. Fin[d], A. Genre[e], C. Prandi[a]

[a]Dipartimento di Chimica, NIS Interdepartmental Centre, Università di Torino, Via Pietro Giuria 7, 10125, Torino, Italy. *Fax: +39 011 670 7855; Tel: +39 011 670 7943; E-mail: claudio.garino@unito.it*
[b]University of Freiburg, Faculty of Biology, Cell Biology, Schänzlestr. 1, 79104 Freiburg, Germany
[c]Aix-Marseille Université, CNRS, ICR (UMR 7273), 13013 Marseille, France
[d]Department of Chemistry and Biochemistry, University of California, San Diego 9500 Gilman Drive, La Jolla, CA 92093-0358 (USA)
[e]Dipartimento di Scienze della Vita e Biologia dei Sistemi, Università di Torino, Viale Mattioli 25, 10125, Torino, Italy.

Keywords: imidazo[1,5-a]pyridine, imidazo[5,1-a]isoquinoline, luminescence, large Stokes' shift, cell imaging, fluorescence labelling

Abstract

A series of new dyes based on the fluorescent imidazo[1,5-a]pyridine moiety has been designed and synthesized specifically for fluorescence cell imaging application. The obtained molecules contain a carboxylic functional group inserted to increase the water solubility and to provide an effective conjugation site. Their structural and optical properties have been deeply investigated and compared with theoretical calculations. The suitability of the products as fluorescent labels for cell imaging applications has been investigated by laser scanning confocal microscopy, both *in vivo* on *Arabidopsis thaliana* seedlings and *in vitro*, on mouse fibroblast cells. The compounds displayed good permeability to the plant cell wall and plasma membrane, they were efficiently internalized in the inner plant tissues, and retained a strong fluorescence in aqueous media.

1. Introduction

Practical and tuneable fluorophores with suitable photophysical properties are necessary components for the development of photosensitizers, photonic materials and optical chemosensors. Furthermore, chemically synthesized luminescent probes are critical tools in biology and medicine to visualize and decipher the activity of cells, tissues, organs and whole organisms [1–3].

Heteroaromatic imidazo[1,5-a]pyridine and its derivatives have gained widespread attention, because of their pharmaceutical (HIV-protease inhibitors, 5-HT4 receptor partial agonists in Alzheimer's disease, etc.) [4–8], chemical (N-heterocyclic carbene chemistry [9–11], ligands in coordination chemistry [12–19], pH-probes [20–22]) and technological (organic light-emitting diodes, thin-layer field effect transistors, down-shifting luminescent layers) [23–25] applications. On the other hand, due to the essential structural flexibility and notable optical properties, imidazo[1,5-a]pyridines represent excellent candidates to be widely studied for different applications. The distinctive emission of the imidazo[1,5-a]pyridine moiety typically lies in the 450–530 nm range, with large Stokes' shift (about 100 nm).

Recent synthetic successes and promising optical properties prompted us to further explore the class of imidazo[1,5-a]pyridine derivatives by introducing a chemical group suitable for conjugation and optical tunability.

Herein, we report the synthesis and characterization of new water-soluble 1,3 substituted imidazo[1,5-a]pyridines and 1,3 substituted imidazo[5,1-a]isoquinoline dyes (Figure 1, Scheme S1) and their application in fluorescence cell imaging. The integration of imidazo[1,5-a]pyridine / isoquinoline units leads to novel dye structures with promising properties that may be considered for a further development of functional fluorophores, readily obtainable by a direct and inexpensive three component coupling.

The fluorophores have been designed to explore the relationship between chemical and electronic structure, preserving the prerequisite for fluorescence microscopy application. Fluorescent probes for biological applications must exhibit good water solubility, high quantum yield, high molar extinction coefficients (ε) and a chemical group suitable for conjugation with targeting ligands to obtain potential biomarker systems, requirements which further highlight the on-going challenges in this area.

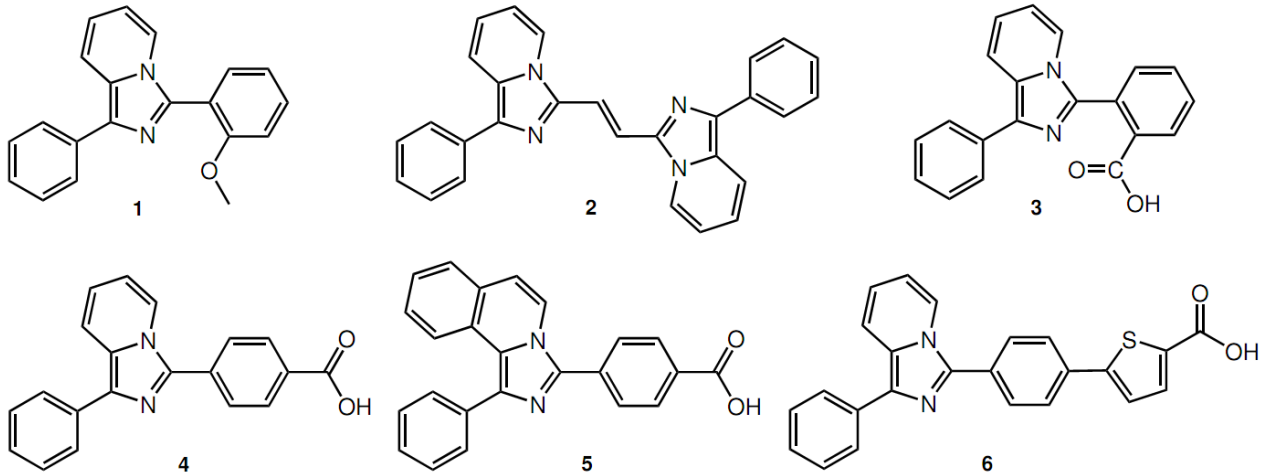

Fig. 1. Chemical structures of investigated compounds.

2. Results and discussion

Compound **1** and **2** have been chosen due to their photophysical properties, based on previous works reporting the optical properties of imidazo[1,5-a]pyridine dyes [25–27]. **1** is characterized by a high emission quantum yield (38%) while **2** is the most bathochromic member of the series (structured emission with maximum at 490 nm and shoulders at 523 and 565 nm), an optical characteristic particularly appreciated in confocal microscopy applications. The new fluorophores (**3–6**) have been designed bearing a carboxylic functional group to increase the water solubility and to provide a conjugation site.

We have adopted two distinct synthetic strategies to modulate the properties of these fluorescent bio-probes. A carboxylic function was introduced at different positions along the molecular skeleton to confer hydrophilicity and provide a further reaction site. In parallel, the imidazo[1,5-a]pyridine π-system was extended to red-shift the photophysical properties of the new probes.

2.1. Synthesis

Compound **1**–**6** are based on the fluorescent imidazo[1,5-a]pyridine structure, obtained by one-pot cyclization through two different synthetic approaches [28,29]. Compound **1** [25] and **3**–**6** were prepared by condensation of substituted phenyl ketones and aromatic aldehydes in acetic acid and ammonium acetate (Scheme S1). Compound **2** was synthesised by condensation of phenyl(pyridin-2-yl)methanamine and maleic acid with propylphosphonic anhydride (T3P) in *n*-butyl acetate [26].

The structural modification of **1**, by replacing a methoxy with a carboxy group, was achieved employing 2-formyl-benzoic acid. Surprisingly, the optical properties of the resulting product **3** are below expectation and do not reflect those of **1**. Thus, employing 4-formyl-benzoic acid instead of 2-formyl-benzoic acid we changed the substitution on the phenyl substituent in position 3 of the imidazo[1,5-a]pyridine from *ortho* (**3**) to *para* (**4**) position, partially recovering the optical properties. To further improve these properties, we extended the π-system into imidazo[1,5-a]pyridine core that should affect the photophysical properties obtaining a favourable bathochromic effect. To this goal, compound **5** was synthetized by introducing on the 1-phenylimidazo[1,5-a]pyridines core an additional aryl ring in position 7, 8 using 1-isoquinolinyl phenyl methanone instead of phenyl(pyridin-2-yl)methanone. The optical properties of **5** reveal an increased quantum yield but an unexpected hypsochromic shift. An alternative strategy to extend the π-system was achieved by introducing a thiophene moiety on the position 3 of the imidazo[1,5-a]pyridine core. Various probes containing thiophene motif in their structures show a wide range of interesting photophysical properties [30–34]. An organohalide derivate suitable for Suzuki cross coupling was prepared by reacting 4-bromo-benzaldehyde and phenyl(pyridin-2-yl)methanone. The obtained 3-(4-bromophenyl)-1-phenylH-imidazo[1,5-a]pyridine intermediate was coupled with a thiophene-2-carboxylic boronic acid, obtaining **6**.

2.2 Optical characterization

High molar extinction coefficient, good absorption fingerprint in a defined spectral region and efficient emission properties with great quantum yield and large Stokes' shifts are fundamental requirements for any fluorophore designed to be used in confocal microscopy.

The new substituted 1-phenylimidazo[1,5-a]pyridines are characterized by absorption maxima below 460 nm and emission bands in the range between 470 and 520 nm, describing a large Stokes' shift, as can be seen in Table 1.

Table 1. Electronic absorption and emission properties of **1**–**6** measured in acetonitrile and in aqueous solutions.

Compound	λ_{abs} (nm)	log ε	λ_{em} (nm)		ϕ %		τ (ns)
			CH_3CN	H_2O	CH_3CN	H_2O	
1[a]	305 374	4.37 3.90	479	475	38	27	7.5
2[b]	465 438 308	4.35 4.45 4.26	523 491	–	10	–	1.0
3	302 357	4.02 3.84	494	461	2	< 1	5.5
4	302 372	4.29 4.38	501	483	13	12	1.5
5	353	4.17	473	460	38	42	2.5
6	305 362	3.73 3.59	485	471	44	15	1.5

[a] spectroscopic data from ref [25], [b] spectroscopic data from ref [26].

2.2.1 Absorption properties

The absorption peaks of **1**–**6** are in the wavelength range between 250 nm and 460 nm. The compounds present two main absorption bands, one in the 300–320 nm range (except compounds **2**) and a second one centred at 360–380 nm (Figure 2). The first band shows greater values of the molar extinction coefficient, as previously reported for 1,3 substituted imidazo[1,5-a]pyridines [14,15,35,36].

The absorption spectra of the investigated compounds are essentially originated from π–π* electronic transitions, even if a limited intramolecular charge-transfer character is present for the transitions at higher energy, as emerged by comparing the experimental and the calculated spectra (Fig. 3 and Fig. S2–5 in the Supplementary Information file).

The various substituents in position 3 on the imidazo[1,5-a]pyridine moiety have a limited effect on the absorption bands. However, it is evident that replacing the electron-donating group (i.e. $–OCH_3$ in **1**) with the electron-withdrawing groups (i.e. –COOH in **3** and **4**) on the phenyl substituent in position 3 induces a new lowest energy electronic transition, having a marked charge-transfer character from the rest of the molecule to the substituents in position 3 (see Fig. 3 for **1** and **3** and Figs. S3–5). Comparison of the absorption behaviour of **3** and **4** highlights a bathochromic shift and an intense increase of the molar extinction coefficients, confirmed by calculations (Figs. 3 and S3).

The absorption properties do not significantly change extending the imidazo[1,5-a]pyridine (**4**) to the imidazo[5,1-a]isoquinoline core (**5**). The π-system extension due to the addition of the aryl ring in position 7, 8 of the imidazo[1,5-a]pyridine moiety does not provide the desired bathochromic effect.

DFT calculations explain this experimental result, evidencing a limited role of the additional aromatic ring in the electronic transitions of **5**, in particular in the lowest energy one (Fig. S4). The

introduction of the thiophene moiety in **6** has evident effects on the emission properties although it does not modify the typical absorption profile of 1,3 substituted imidazo[1,5-a]pyridines.

Compounds **4**–**6** show similar absorption maxima, suggesting that the π-system extension of the imidazo[1,5-a]pyridine core does not affect significantly the absorption properties of such molecules. Nevertheless, the conjugation extension obtained linking two imidazo[1,5-a]pyridines with a trans-1,2-ethylene (**2**) provided a strong bathochromic effect (80 nm), associated with a peculiar absorption profile, if compared with the other imidazo[1,5-a]pyridines. However, in the case of **2**, the chromogenic core is constituted by a conjugated system centred on the trans-1,2-ethylene moiety and extended on the two adjacent imidazole rings, with only marginal contribution from the rest of the molecule, in particular for the lowest energy electronic transition.

All the compounds display an hypsochromic effect when evaluated in aqueous solution (see Table 1 and Figure S1, with the exception of **2** that is insoluble). The effect is moderate for **1** and **6** and more pronounced (about 20 nm) for **4** and **5**.

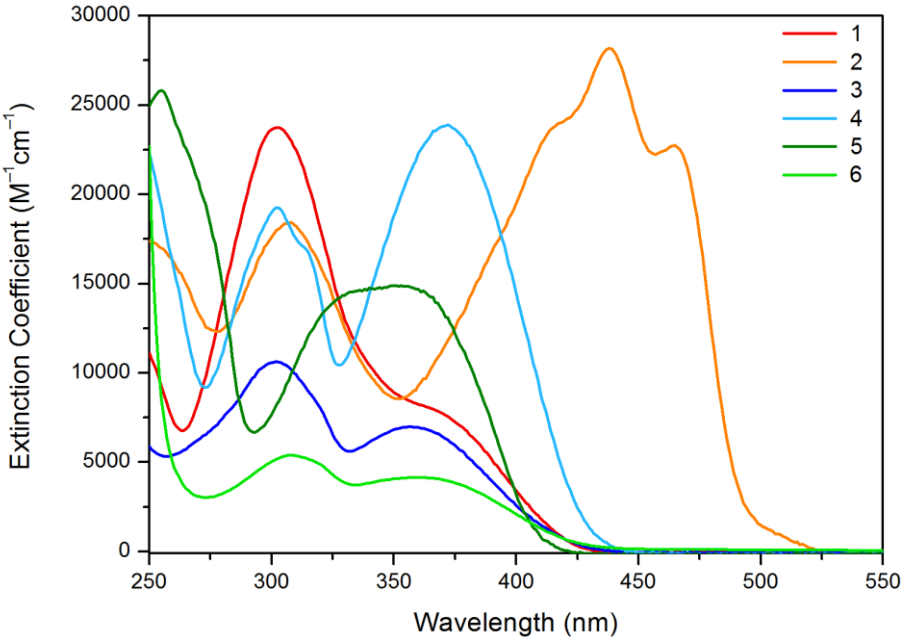

Fig. 2. Experimental electronic absorption spectra of **1**–**6** recorded in acetonitrile solution.

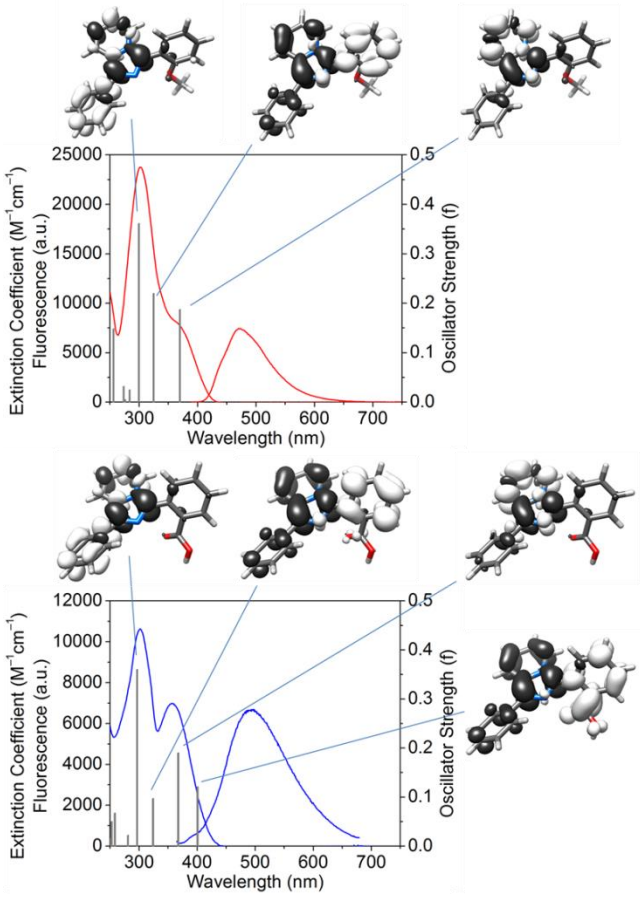

Fig. 3. Experimental electronic absorption (left) and emission (right) spectra of **2** (top) and **3** (bottom) in acetonitrile solution together with calculated singlet excited state transitions (vertical bars with height equal to the oscillator strength (f) values). Electron Density Difference Maps (EDDMs) for selected TDDFT singlet transitions (black indicates a decrease in electron density while white indicates an increase).

2.2.2 Emission properties

The emission spectra of **1**–**6** in acetonitrile solution are showed in Figure 4 and the emission wavelengths are reported in Table 1. The probes show an emission band centred between 470 nm and 520 nm.

Compounds **3** and **4**, differing only for the position of the carboxylic group, were synthesized to evaluate a possible Excited-State Intramolecular Proton Transfer (ESIPT) effect with the imidazo[1,5-a]pyridine core. However, the comparison among quantum yields and emission spectra of **1**, **3**–**5** highlighted the absence of interactions between the nitrogen in position 2 of the imidazo[1,5-a]pyridine nucleus and the functional group present in position 3. The same evidence has been previously reported by us comparing four different 3-substituited imidazo[1,5-a]pyridines, bearing $–OCH_3$ and –OH groups. The quantum yield of **4** dramatically increases if compared with **3**, for this reason **5** and **6** have been designed keeping the substitution in *para* position of the 3-phenyl-1-phenylH-imidazo[1,5-a]pyridine core.

The new derivatives designed for biofunctionalization show a moderate bathochromic shift of about 15 nm compared to **1**. Their quantum yields in acetonitrile solution drop to 2% for **3** and gradually recover (**4** ϕ = 13%, **5** ϕ = 38%) until overcome 44% (compound **6**) which, to the best of our knowledge, is also the highest value reported in literature among imidazo[1,5-a]pyridines.

In aqueous solution (see Table 1 and Figure 4), the new compound **3**–**6** show an hypsochromic effect of about 20 nm. The emission quantum yield remains unchanged, within the experimental error, for **3**–**5** and decreases for **6**.

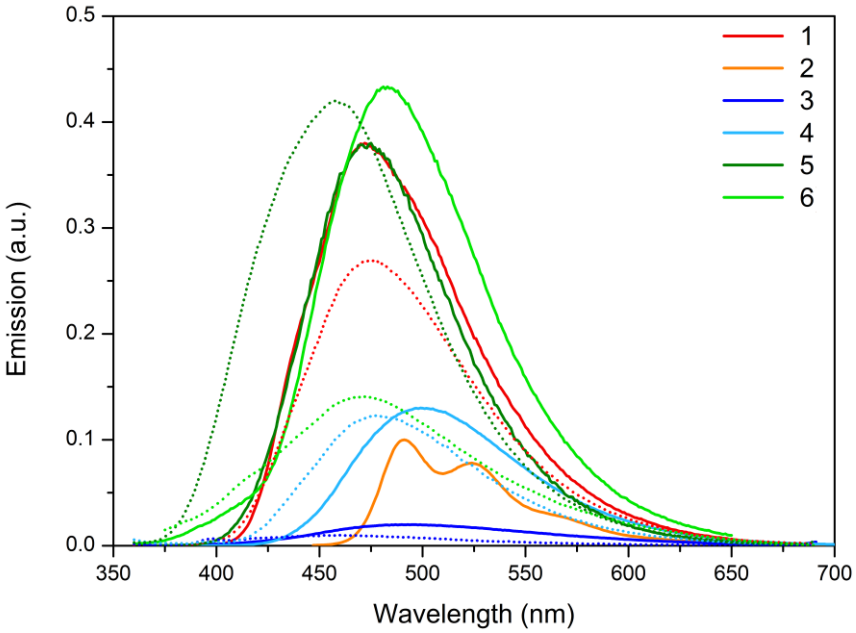

Fig. 4. Experimental emission spectra of **1**–**6** recorded in acetonitrile (solid lines) and in aqueous (dotted lines) solutions.

2.3 Crystal Structure

Yellow/orange prismatic crystals of **4** were obtained from a saturated dichloromethane solution by slow evaporation at room temperature into a NMR tube.

Compound **4** crystallizes in $P2_1/n$ space group and a molecule of the solvent has been maintained into the crystal structure (Figure 5). The structural solvent is disordered by the typical two component disorder and does not participate to any of the stronger interaction of the structure. The complete molecule of **4** is present into the asymmetric unit.

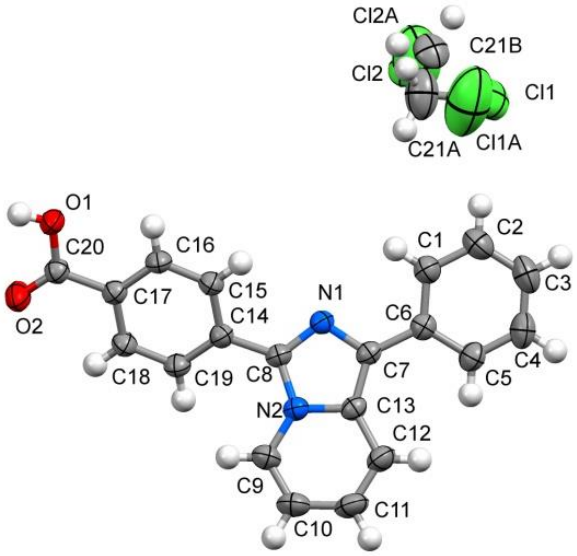

Fig. 5. Asymmetric unit of **4**. Only the numeration of non-hydrogen atoms is shown for clarity. (Probability level for thermal ellipsoids: 50%).

The torsion of the para-substituted ring respect to the central imidazo[1,5-a]pyridine backbone is higher compared to most of the other structures of the family of diaryl imidazo[1,5-a]pyridines (–30.47(10)°) [26,37]: the other reported molecules are usually coplanar, however **4** has an acidic substituent that acts as a strong hydrogen bond donor through the central N1 nitrogen forming a strong interaction (d(N1···O1) = 2.616(5) Å and d(N1···H1a) = 2.889(6) Å) that can bend the structure. By comparison, it is interesting to notice that specific localized interactions can rotate the lateral rings in this family of compounds; this is also the case for the structure 3-(anthracen-9-yl)-1-phenylimidazo[1,5-a]pyridine, in which the formation of a typical paddlewheel architecture for the lateral anthracenic substituent imposes a rotation respect to the central backbone [25] or for 2-(1-(pyridin-2-yl)imidazo[1,5-a]pyridin-3-yl)phenol [19] that shows for a lateral OH···N interaction a torsional angle of 64.94(11)°. The other factor that can modify this geometry is the presence of particularly crowded lateral rings; for example 3-(2-methylphenyl)-1-(pyridin-2-yl)imidazo[1,5-a]pyridine [19] that shows a torsional angle of 71.06(10)° between the central ring and the methylated phenyl substituent. The carboxyl substituent lies on the same plane of the bonded ring, while the imidazo[1,5-a]pyridine backbone of the interacting molecule is nearly perpendicular to it (85.6(1)° of torsional angle between the two rings) and bent of 22.97(15)° with respect to the axis of the other molecule passing to the bond C17-C20. This hydrogen interaction repeated for each couple of molecules form a supramolecular wavy chain connected by strong hydrogen interactions with a graph structure of $C^1_1(9)$ (Figure 6) [38]. A similar pattern can be found in the structure of 2-(1-(pyridin-2-yl)imidazo[1,5-a]pyridin-3-yl)phenol [19] but with a less pronounced wavelength for the *orto* position of the hydroxyl group on the phenyl substituent. There is no presence of π–π interactions, probably due to the bulkiness of the substituents and to the presence of the disordered solvent that isolate the chains, as was reported for 3-(1H-indol-3-yl)-1-phenylimidazo[1,5-a]pyridine [25]. Another strong hydrogen bond donor centre bearing molecule, pyridin-2-yl(3-(pyridin-2-yl)imidazo[1,5-a]pyridin-1-yl)methanol [39], forms a hydrogen bond supported chain between the OH lateral group and the central imidazolic nitrogen, but the geometry of the molecule and probably a greater tendency to π–π interactions bring to the formation, in that case, of a linear rigid supramolecular polymer.

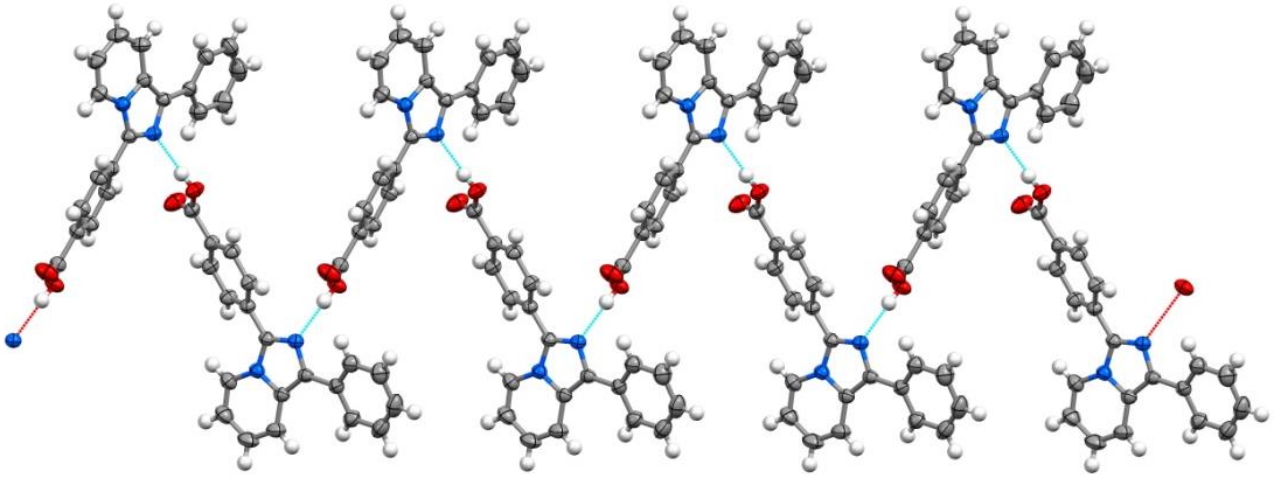

Fig. 6. Hydrogen bond-based chain in the structure of **4** (Probability level for thermal ellipsoids: 50%).

2.4. Confocal microscopy

To investigate the suitability of these newly synthesized compounds as fluorescent labels for cell imaging applications, *Arabidopsis thaliana* seedlings were incubated for 5 minutes with each molecule (10 μM aqueous solution) and immediately *in vivo* imaged with a laser scanning confocal microscope. In order to avoid the intense fluorescence of chlorophyll, confocal imaging was only performed on roots. It is worth noting that, while compounds **1**–**5** could be readily dissolved in water containing 0.1% acetone, compound **6** could only be dissolved in water containing 1% DMSO.

Fluorescence emission spectra were recorded (λ_{exc} = 405 nm, see Figure S6 Supplementary Information file), and the obtained emission maxima for compounds **1**–**6** are in accordance with the spectroscopic data measured in solution (Figure 4). Compounds **1**, **4** and **6** displayed good permeability to the plant cell wall and plasma membrane, a critical feature in fluorophores to be used as *in vivo* probes: they were efficiently internalized in the inner plant tissues, and retained a strong fluorescence in aqueous media (Figure 7). The fluorescent signal detected for compounds **2**, **3**, and **5** was weaker, probably due to a reduced ability of these compounds to penetrate and/or accumulate inside the living plant tissues or because of the aqueous environment, which can affect the optical properties of fluorescent molecules [1] (Figure 7). However, these compounds were effective in distinctly labelling the cytoplasm of mouse fibroblast cells *in vitro* (Figure S7 Supplementary Information file) and therefore can be suitable as counterstain to provide contrast in multi-colour fluorescence microscopy.

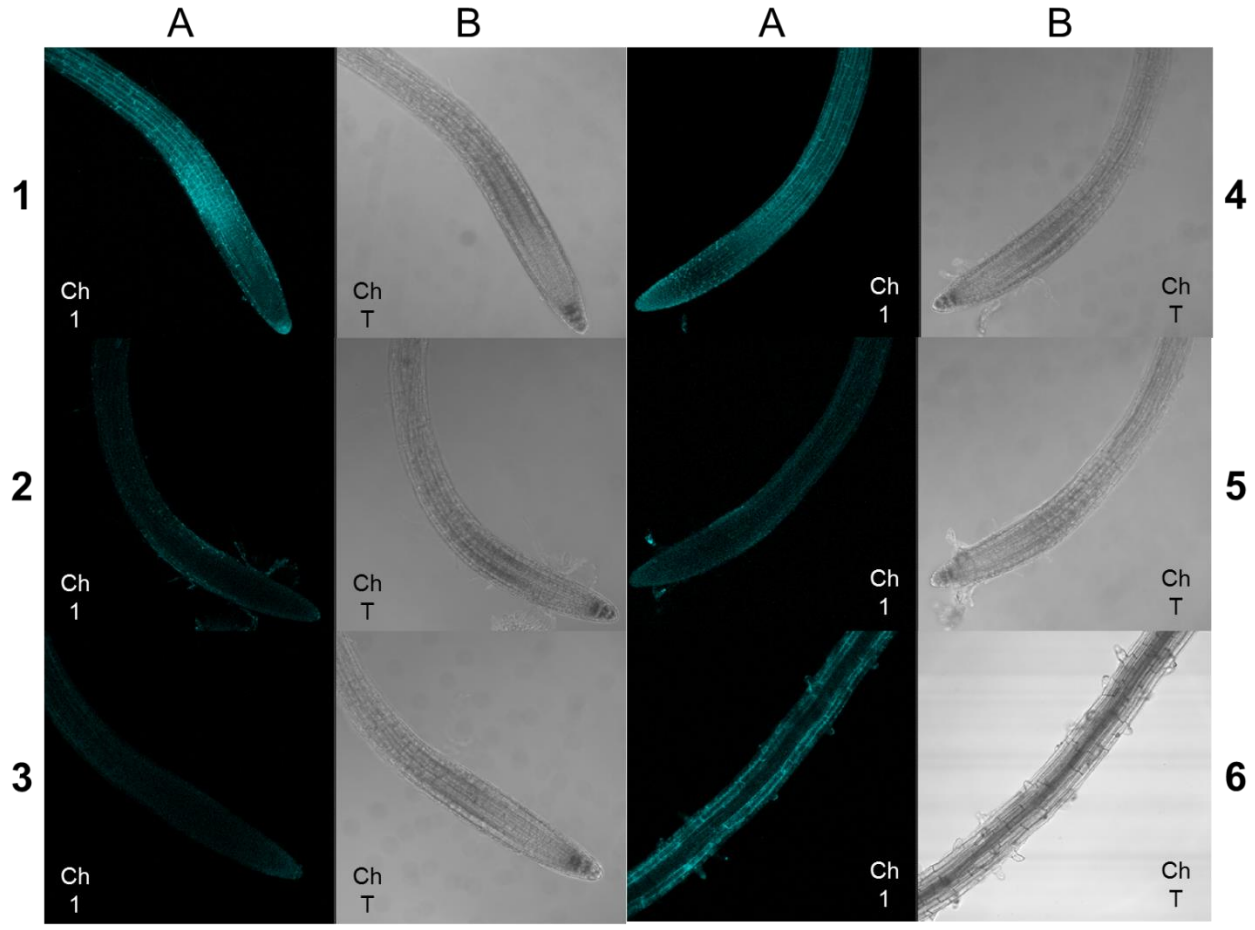

Fig. 7. Fluorescence (A) and transmitted light (B) confocal images showing *Arabidopsis thaliana* root after 5 min incubation with a 10 μM aqueous solution of **1**–**6**.

3. Experimental details

3.1 Materials and techniques

All solvents and raw materials were used as received from commercial suppliers (Sigma-Aldrich and Alfa Aesar) without further purification. 5-(4,4,5,5-tetramethyl-1,3,2-dioxaborolan-2-yl)thiophene-2-carboxylic acid [40], **1** [25] and **2** [26] were prepared as previously reported.

TLC was performed on Fluka silica gel TLC-PET foils GF 254, particle size 25 nm, medium pore diameter 60 Å. Column chromatography was performed on Sigma-Aldrich silica gel 60 (70-230 mesh ASTM).

^{1}H and ^{13}C NMR spectra were recorded on a Bruker Avance 200 spectrometer (^{1}H NMR operating frequency 200 MHz) and on a JEOL ECP 400 spectrometer (^{1}H NMR operating frequency 400 MHz), with chemical shifts referenced to residual protons of the solvent. The following abbreviations are used: s (singlet), d (doublet), t (triplet), dd (doublet of doublets), m (multiplet).

Mass spectra were recorded on a Thermo-Finnigan Advantage Max Ion Trap Spectrometer equipped with an electrospray ion source (ESI) in positive and negative ion acquiring mode.

The single-crystal data were collected with a Gemini R Ultra diffractometer with graphite-monochromated Mo-K_α radiation (λ = 0.71073) by the ω-scan method. The cell parameters were retrieved with the CrysAlisPro software [41], and the same program was used to perform data reduction with corrections for Lorenz and polarizing effects. Scaling and absorption corrections were applied through the CrysAlisPro multiscan technique. All structures were solved with direct methods by using SHELXS-97 [42] and refined with full-matrix least-squares techniques on F^2 with SHELXL-97. All non-hydrogen atoms were refined anisotropically. Hydrogen atoms were calculated and riding on the corresponding atom. CCDC 1824635 contains the supplementary crystallographic data for this paper. These data can be obtained free of charge from The Cambridge Crystallographic Data Centre.

UV-Vis absorption spectra were recorded on a Cary60 spectrometer. Photoemission spectra, luminescence lifetimes and quantum yields were acquired with a HORIBA Jobin Yvon IBH Fluorolog-TCSPC spectrofluorometer, equipped with a Quanta-φ integrating sphere. The spectral response was corrected for the spectral sensitivity of the photomultiplier. Luminescence lifetimes were determined by time-correlated single-photon counting; excitation was achieved with nanosecond pulses generated by NanoLED pulsed diodes. Emission-decay data were collected in 2048 channels to 10000 counts in the peak channel and analysed with the software DAS6 (TCSPC decay-analysis software).

3.2 Syntheses

3.2.1 General one-pot cyclization procedure

A mixture containing 1.0 mmol of phenyl(pyridin-2-yl)methanone (for compounds **3**, **4** and 3-(4-bromophenyl)-1-phenylH-imidazo[1,5-a]pyridine) or isoquinolin-1-yl-phenyl-methanone (for compounds **5** and 3-(4-bromophenyl)-1-phenylH-imidazo[5,1-a]isoquinoline), 1.1 mmol of appropriate aldehyde and 5 mmol of ammonium acetate was heated in 25 mL of glacial acetic acid at reflux for 12 h. After cooling the reaction mixture to room temperature, the acetic acid was removed by vacuum distillation. The solid was dissolved and neutralized in Na_2CO_3 aqueous solution and the mixture extracted with CH_2Cl_2. The organic layer was separated and the solvent

evaporated under vacuum. The crude solid was washed several times with diethyl ether and dried under vacuum obtaining the product as a yellow powder.

3.2.2 4-(1-phenylH-imidazo[1,5-a]pyridin-3-yl)benzoic acid (**3**)
1.0 mmol of phenyl(pyridin-2-yl)methanone and 1.1 mmol of 4-formyl-benzoic acid. Yield: 281 mg, 89.5%, MS (ESI): m/z 315.11 [$(M+H)^+$], 313.33 [$(M–H)^–$]. ^{1}H NMR (200 MHz, DMSO): δ = 13.12 (s, 1H), 8.60 (d, J = 7.0 Hz, 1H), 8.04 (m, 7H), 7.48 (t, J = 8.0 Hz, 2H), 7.31 (t, J = 8.0 Hz, 1H), 7.02 (t, J = 6.0 Hz, 1H), 6.84 (t, J = 6.0 Hz, 1H) ppm; ^{13}C NMR (50 MHz, DMSO): δ = 167.7, 136.3, 134.5, 133.7, 131.2, 130.2, 130.0, 128.8, 128.1, 127.6, 126.5, 126.2, 122.8, 121.5, 118.7, 114.3 ppm.

3.2.3 2-(1-phenylH-imidazo[1,5-a]pyridin-3-yl)benzoic acid (**4**)
1.0 mmol of phenyl(pyridin-2-yl)methanone and 1.1 mmol of 2-formyl-benzoic acid. Yield: 180 mg, 57.3%, MS (ESI): m/z 315.08 [$(M+H)^+$], 313.33 [$(M–H)^–$]. ^{1}H NMR (200 MHz, Acetone): δ = 8.15 (d, J = 16.0 Hz, 1H), 7.97 (m, 3H), 7.73 (m, 4H), 7.44 (t, J = 8.0 Hz, 2H), 7.25 (t, J = 8.0 Hz, 1H), 6.90 (m, 1H), 6.63 (t, J = 8.0 Hz, 1H) ppm; ^{13}C NMR (50 MHz, Acetone): δ = 167.7, 138.1, 136.2, 133.1, 132.9, 132.6, 131.7, 131.2, 131.1, 130.3, 129.4, 127.8, 127.0, 126.8, 123.2, 121.1, 119.2, 113.6 ppm.

3.2.4 4-(1-phenylH-imidazo[5,1-a]isoquinolin-3-yl)benzoic acid (**5**)
1.0 mmol of isoquinolin-1-yl-phenyl-methanone and 1.1 mmol of 2-formyl-benzoic acid. Yield: 151 mg, 41.5 %, MS (ESI): m/z 365.40 [$(M+H)^+$], 363.39 [$(M–H)^–$]. ^{1}H NMR (200 MHz, DMSO): δ = 13.15 (s, 1H), 8.28 (d, J = 8.0 Hz, 1H), 8.05 (m, 4H), 7.61 (m, 9H), 7.07 (d, J = 6.0 Hz, 1H) ppm; ^{13}C NMR (50 MHz, DMSO): δ = 166.9, 138.7, 136.0, 135.3, 133.4, 130.7, 130.0, 129.5, 128.6, 128.3, 127.6, 127.5, 124.6, 124.0, 121.7, 114.6 ppm.

3.2.5 3-(4-bromophenyl)-1-phenylH-imidazo[1,5-a]pyridine
1.0 mmol of phenyl(pyridin-2-yl)methanone and 1.1 mmol of 4-bromo-benzaldehyde. Yield: 253 mg, 72.4 %, MS (ESI): m/z 350.23 [$(M+H)^+$]. ^{1}H NMR (200 MHz, $CDCl_3$): δ = 7.78 (d, J = 8.0 Hz, 1H), 7.52 (d, J = 6.0 Hz, 2H), 7.44 (d, J = 10.0 Hz, 1H), 7.29 (m, 4H), 7.08 (t, J = 8.0 Hz, 2H), 6.91 (m, 1H), 6.40 (m, 1H) , 6.19 (t, J = 8.0 Hz, 1H) ppm; ^{13}C NMR (50 MHz, $CDCl_3$): δ = 137.0, 134.8, 132.3, 130.3, 129.8, 129.1, 128.9, 128.0, 126.9, 126.8, 122.9, 121.6, 120.0, 119.4, 113.8 ppm.

3.2.6 5-(4-(1-phenylH-imidazo[1,5-a]pyridin-3-yl)phenyl)thiophene-2-carboxylic acid (**6**)
A solution of 3-(4-bromophenyl)-1-phenylH-imidazo[1,5-a]pyridine (0.7 mmol), 5-(4,4,5,5-tetramethyl-1,3,2-dioxaborolan-2-yl)thiophene-2-carboxylic acid (1.7 mmol) and K_3PO_4 (3.0 mmol) in anhydrous THF (20 mL) was thoroughly degassed by bubbling nitrogen for 15 minutes. Then, $Pd(PPh_3)Cl_2$ (10%) was added under nitrogen and the resulting solution was degassed for further 5 minutes. The reaction mixture was stirred at reflux (80 °C) overnight. After cooling down, the reaction was quenched with HCl 1 M (5 mL) and the product was extracted with CH_2Cl_2 (3 x 30 mL). The combined organic phases were washed with brine, dried over anhydrous Na_2SO_4 and the solvent was removed under reduced pressure. The crude product was purified by column chromatography (CH_2Cl_2/MeOH 92/8) to give the final product **6** as a dark yellow solid. Yield: 168 mg, 63%, MS (ESI): m/z 397.47 [$(M+H)^+$], 395.45 [$(M–H)^–$]. ^{1}H NMR (400 MHz, DMSO): δ = 8.55 (d, J = 7.2 Hz, 1H), 8.02 (d, J = 9.2 Hz, 1H), 7.94 (m, 4H), 7.83 (d, J = 8.5 Hz, 2H), 7.47 (m, 3H), 7.29 (m, 2H), 6.99 (dd, 1H), 6.81 (t, J 6.5 Hz, 1H) ppm.

3.3 Confocal microscopy

Seeds of *Arabidopsis thaliana* wild type (WT; Columbia; Col-0) were surface sterilized and germinated on half-strength Murashige and Skoog (MS) plates supplemented with 1.5% (w/v) sucrose and 1% agar (w/v). Plates were incubated vertically in the dark at 4 °C for 2 days to synchronize germination. Plates were then positioned in an upright 45° position, and incubated at 22 °C. Light intensity at plate level was 50–60 μE m^{-2} s^{-1} provided by white fluorescent tubes with a photoperiod of 16/8 h (light/dark) for 6 d.

For confocal observations, the roots of 6-d-old seedlings were incubated 5 minutes in 10 μM aqueous solution of each distinct fluorophore **1**–**6** (10 mM acetone stock for compounds **1**–**5**, 1 mM DMSO stock for compound **6**), quickly rinsed in water and then gently transferred to slides using forceps. After adding a drop of water and a coverslip, seedlings were immediately imaged with a Leica TCS SP2 confocal microscope using both a 20x magnification objective and a long-distance 40X water-immersion objective (HCX Apo 0.80). Emission spectra (430–800 nm) were obtained by lambda scan mode (10 nm emission window and step size = 6.66 nm) on *Arabidopsis thaliana* roots excited at 405 nm with a laser diode. Based on the recorded maximum emission for each fluorophore, an emission window of 450–550 nm was chosen to visualize fluorescence and distribution *in vivo*; the parameters of the photomultiplier tube detector (PMT) were kept uniform between experiments to allow the comparison of fluorescence intensities.

3.4 Computational Details

All calculations were performed with the Gaussian 09 (G09) program package [43], employing the Density Functional Theory (DFT) and its Time-Dependent extension TD-DFT [44,45]. The Becke three-parameter hybrid functional [46], and the Lee−Yang−Parr's gradient corrected correlation functional (B3LYP) [47] were used together with the 6-31G** basis set [48]. The solvent effect was included using the polarizable continuum model (CPCM method) [49,50], with acetonitrile as solvent. Geometry optimizations were carried out without any symmetry constraints, the nature of all stationary points was verified via harmonic vibrational frequency calculations. No imaginary frequencies were found, indicating we had located minima on potential energy surfaces. The UV-Vis electronic absorption spectra were simulated by TD-DFT [44,45], computing a total of 64 singlet excited states. The electronic distribution and the localization of the singlet excited states were visualized using Electron Density Difference Maps (EDDMs). GaussSum 2.2.5 [51] was used to simulate the theoretical UV–Vis spectra and for EDDMs calculations [52,53]. Molecular-graphic images were produced by using the UCSF Chimera package from the Resource for Biocomputing, Visualization, and Informatics at the University of California, San Francisco [54].

4. Conclusions

A series of new fluorescent 1,3 substituted imidazo[1,5-a]pyridine and imidazo[5,1-a]isoquinoline derivatives has been synthesized, structurally and electronically characterized and preliminary tested for application as fluorescent probes for cell imaging.

The luminescent imidazo[1,5-a]pyridine core has been successfully derivatized with designed substituents bearing a carboxylic group suitable for conjugation, employing a convenient and highly accessible synthetic approach, in high yields, preserving stability and water solubility.

The structure of the obtained compounds was determined by ^{1}H NMR, ^{13}C NMR, X-Ray Diffraction and Electrospray Ionization Mass Spectrometry. Electronic absorption and emission spectra of the compounds were investigated and compared with theoretical calculations.

The position of the carboxylic group, conveniently introduced for biofunctionalization, strongly modify the optical properties. The 3-aryl substitution on imidazo[1,5-a]pyridine derivatives markedly affects the photophysical properties, while the extension of the π-system due to the addition of the aryl ring in position 7, 8 of the imidazo[1,5-a]pyridine core has unexpectedly a limited effect, as confirmed by DFT calculations.

The comparison of the photophysical properties induced by the structural modification on the imidazo[1,5-a]pyridine nucleus, assisted by computational modelling, led us throughout the synthesis of the series **1**–**6**. This allowed to increase the emission quantum yield from 2 to 44 % and evidenced a strong dependency of the emission properties on the chemical structure; a meaningful observation for planning future imidazo[1,5-a]pyridine derivatives.

In summary, new water-soluble fluorescent dyes have been developed and their potential applicability to *in vivo* and *in vitro* cell fluorescence imaging has been confirmed. These luminescent products have some distinct advantages including easy preparation, notable emission, and large Stokes' shift, which is of benefit in fluorescence microscopy to minimize cross-talk between the excitation source and the fluorescent emission. They can be used both as such or conjugated as luminescent labels in more complex biomarker systems.

On the basis of these promising properties, further studies are in progress to test these derivatives as tuneable low-cost fluorescent materials.

References

[1] T. Terai, T. Nagano, Pflüg. Arch. - Eur. J. Physiol. 465 (2013) 347–359.

[2] X. Zhang, X. Zhang, B. Yang, Y. Zhang, Y. Wei, Acs Appl. Mater. Interfaces 6 (2014) 3600–3606.

[3] G. Xie, C. Ma, X. Zhang, H. Liu, L. Yang, Y. Li, K. Wang, Y. Wei, Dyes Pigments 143 (2017) 276–283.

[4] D. Kim, L.P. Wang, J.J. Hale, C.L. Lynch, R.J. Budhu, M. MacCross, S.G. Mills, L. Malkowitz, S.L. Gould, J.A. DeMartino, M.S. Springer, D. Hazuda, M. Miller, J. Kessler, R.C. Hrin, G. Carver, A. Carella, K. Henry, J. Lineberger, W.A. Schleif, E.A. Emini, Bioorg. Med. Chem. Lett. 15 (2005) 2129–2134.

[5] L.J. Browne, C. Gude, H. Rodriguez, R.E. Steele, A. Bhatnager, J. Med. Chem. 34 (1991) 725–736.

[6] B.P. Fauber, A. Gobbi, K. Robarge, A. Zhou, A. Barnard, J. Cao, Y. Deng, C. Eidenschenk, C. Everett, A. Ganguli, J. Hawkins, A.R. Johnson, H. La, M. Norman, G. Salmon, S. Summerhill, W. Ouyang, W. Tang, H. Wong, Bioorg. Med. Chem. Lett. 25 (2015) 2907–2912.

[7] R. Nirogi, A.R. Mohammed, A.K. Shinde, N. Bogaraju, S.R. Gagginapalli, S.R. Ravella, L. Kota, G. Bhyrapuneni, N.R. Muddana, V. Benade, R.C. Palacharla, P. Jayarajan, R. Subramanian, V.K. Goyal, Eur. J. Med. Chem. 103 (2015) 289–301.

[8] M.A. Ingersoll, A.S. Lyons, S. Muniyan, N. D'Cunha, T. Robinson, K. Hoelting, J.G. Dwyer, X.R. Bu, S.K. Batra, M.-F. Lin, PLOS ONE 10 (2015) e0131811.

[9] M. Alcarazo, S.J. Roseblade, A.R. Cowley, R. Fernandez, J.M. Brown, J.M. Lassaletta, J. Am. Chem. Soc. 127 (2005) 3290–3291.

[10] C. Burstein, C.W. Lehmann, F. Glorius, Tetrahedron 61 (2005) 6207–6217.

[11] F.E. Hahn, Angew. Chem.-Int. Ed. 45 (2006) 1348–1352.

[12] S.J. Roseblade, A. Ros, D. Monge, M. Alcarazo, E. Alvarez, J.M. Lassaletta, R. Fernandez, Organometallics 26 (2007) 2570–2578.

[13] G. Volpi, C. Garino, L. Salassa, J. Fiedler, K.I. Hardcastle, R. Gobetto, C. Nervi, Chem.- Eur. J. 15 (2009) 6415–6427.

[14] L. Salassa, C. Garino, A. Albertino, G. Volpi, C. Nervi, R. Gobetto, K.I. Hardcastle, Organometallics 27 (2008) 1427–1435.

[15] C. Garino, T. Ruiu, L. Salassa, A. Albertino, G. Volpi, C. Nervi, R. Gobetto, K.I. Hardcastle, Eur. J. Inorg. Chem. (2008) 3587–3591.
[16] N. Kundu, M. Maity, P.B. Chatterjee, S.J. Teat, A. Endo, M. Chaudhury, J. Am. Chem. Soc. 133 (2011) 20104–20107.
[17] N. Kundu, S.M.T. Abtab, S. Kundu, A. Endo, S.J. Teat, M. Chaudhury, Inorg. Chem. 51 (2012) 2652–2661.
[18] Y. Chen, L. Li, Y. Cao, J. Wu, Q. Gao, Y. Li, H. Hu, W. Liu, Y. Liu, Z. Kang, J. Li, Crystengcomm 15 (2013) 2675–2681.
[19] G.A. Ardizzoia, S. Brenna, S. Durini, B. Therrien, M. Veronelli, Eur. J. Inorg. Chem. (2014) 4310–4319.
[20] J.T. Hutt, J. Jo, A. Olasz, C.-H. Chen, D. Lee, Z.D. Aron, Org. Lett. 14 (2012) 3162–3165.
[21] X. Zhang, G.-J. Song, X.-J. Cao, J.-T. Liu, M.-Y. Chen, X.-Q. Cao, B.-X. Zhao, Rsc Adv. 5 (2015) 89827–89832.
[22] G.-J. Song, S.-Y. Bai, X. Dai, X.-Q. Cao, B.-X. Zhao, Rsc Adv. 6 (2016) 41317–41322.
[23] M.D. Weber, C. Garino, G. Volpi, E. Casamassa, M. Milanesio, C. Barolo, R.D. Costa, Dalton Trans. 45 (2016) 8984–8993.
[24] J. Hu, Y. Li, Y. Wu, W. Liu, Y. Wang, Y. Li, Chem. Lett. 44 (2015) 645–647.
[25] G. Volpi, G. Magnano, I. Benesperi, D. Saccone, E. Priola, V. Gianotti, M. Milanesio, E. Conterosito, C. Barolo, G. Viscardi, Dyes Pigments 137 (2017) 152–164.
[26] G. Volpi, C. Garino, E. Priola, E. Diana, R. Gobetto, R. Buscaino, G. Viscardi, C. Barolo, Dyes Pigments 143 (2017) 284–290.
[27] G. Volpi, C. Magistris, C. Garino, Nat. Prod. Res. 0 (2017) 1–8.
[28] J. Wang, R. Mason, D. VanDerveer, K. Feng, X.R. Bu, J. Org. Chem. 68 (2003) 5415–5418.
[29] J.M. Crawforth, M. Paoletti, Tetrahedron Lett. 50 (2009) 4916–4918.
[30] S. Rihn, P. Retailleau, N. Bugsaliewicz, A.D. Nicola, R. Ziessel, Tetrahedron Lett. 50 (2009) 7008–7013.
[31] X. Zhang, H. Yu, Y. Xiao, J. Org. Chem. 77 (2012) 669–673.
[32] R. Gresser, M. Hummert, H. Hartmann, K. Leo, M. Riede, Chem. – Eur. J. 17 (2011) 2939–2947.
[33] Q. Bellier, F. Dalier, E. Jeanneau, O. Maury, C. Andraud, New J. Chem. 36 (2012) 768–773.
[34] S. Parisotto, B. Lace, E. Artuso, C. Lombardi, A. Deagostino, R. Scudu, C. Garino, C. Medana, C. Prandi, Org. Biomol. Chem. 15 (2017) 884–893.
[35] F. Shibahara, R. Sugiura, E. Yamaguchi, A. Kitagawa, T. Murai, J. Org. Chem. 74 (2009) 3566–3568.
[36] F. Shibahara, E. Yamaguchi, A. Kitagawa, A. Imai, T. Murai, Tetrahedron 65 (2009) 5062–5073.
[37] G. Volpi, C. Garino, E. Conterosito, C. Barolo, R. Gobetto, G. Viscardi, Dyes Pigments 128 (2016) 96–100.
[38] J. BERNSTEIN, R. DAVIS, L. SHIMONI, N. CHANG, Angew. Chem.-Int. Ed. 34 (1995) 1555–1573.
[39] T. Murai, E. Nagaya, F. Shibahara, T. Maruyama, Org. Biomol. Chem. 10 (2012) 4943–4953.
[40] I. Palamà, F. Di Maria, I. Viola, E. Fabiano, G. Gigli, C. Bettini, G. Barbarella, J. Am. Chem. Soc. 133 (2011) 17777–17785.
[41] CrysAlisPro Software System, Agilent Technologies UK Ltd., Oxford, U.K., 2007.
[42] G.M. Sheldrick, SHELXL97, University of Göttingen, Göttingen, Germany, 1997.
[43] M.J. Frisch, G.W. Trucks, H.B. Schlegel, G.E. Scuseria, M.A. Robb, J.R. Cheeseman, G. Scalmani, V. Barone, B. Mennucci, G.A. Petersson, H. Nakatsuji, M. Caricato, X. Li, H.P. Hratchian, A.F. Izmaylov, J. Bloino, G. Zheng, J.L. Sonnenberg, M. Hada, M. Ehara, K. Toyota, R. Fukuda, J. Hasegawa, M. Ishida, T. Nakajima, Y. Honda, O. Kitao, H. Nakai, T. Vreven, J. Montgomery, J.E. Peralta, F. Ogliaro, M. Bearpark, J.J. Heyd, E. Brothers, K.N. Kudin, V.N. Staroverov, R. Kobayashi, J. Normand, K. Raghavachari, A. Rendell, J.C. Burant, S.S. Iyengar, J. Tomasi, M. Cossi, N. Rega, N.J. Millam, M. Klene, J.E. Knox, J.B. Cross, V. Bakken, C. Adamo, J. Jaramillo, R. Gomperts, R.E. Stratmann, O. Yazyev, A.J. Austin, R. Cammi, C. Pomelli, J.W. Ochterski, R.L. Martin, K. Morokuma, V.G. Zakrzewski, G.A. Voth, P. Salvador, J.J. Dannenberg, S. Dapprich, A.D. Daniels, Ö. Farkas, J.B. Foresman, J.V. Ortiz, J. Cioslowski, D.J. Fox, Gaussian 09, Gaussian, Inc., Wallingford, CT, 2009.
[44] R.E. Stratmann, G.E. Scuseria, M.J. Frisch, J. Chem. Phys. 109 (1998) 8218–8224.
[45] M.E. Casida, C. Jamorski, K.C. Casida, D.R. Salahub, J. Chem. Phys. 108 (1998) 4439–4449.
[46] A.D. Becke, J. Chem. Phys. 98 (1993) 5648–5652.
[47] C.T. Lee, W.T. Yang, R.G. Parr, Phys. Rev. B 37 (1988) 785–789.
[48] A.D. McLean, G.S. Chandler, J. Chem. Phys. 72 (1980) 5639–5648.
[49] M. Cossi, G. Scalmani, N. Rega, V. Barone, J. Chem. Phys. 117 (2002) 43–54.

[50] S. Miertus, E. Scrocco, J. Tomasi, Chem. Phys. 55 (1981) 117–129.
[51] N.M. O'Boyle, A.L. Tenderholt, K.M. Langner, J. Comput. Chem. 29 (2008) 839–845.
[52] W.R. Browne, N.M. O'Boyle, J.J. McGarvey, J.G. Vos, Chem. Soc. Rev. 34 (2005) 641–663.
[53] M. Headgordon, A.M. Grana, D. Maurice, C.A. White, J. Phys. Chem. 99 (1995) 14261–14270.
[54] E.F. Pettersen, T.D. Goddard, C.C. Huang, G.S. Couch, D.M. Greenblatt, E.C. Meng, T.E. Ferrin, J. Comput. Chem. 25 (2004) 1605–1612.